Bone 55 (2013) 410–417

Contents lists available at SciVerse ScienceDirect

Bone

journal homepage: www.elsevier.com/locate/bone

Original Full Length Article

# Recovery from hind limb ischemia enhances rhBMP-2-mediated segmental bone defect repair in a rat composite injury model

Brent A. Uhrig [a,b], Joel D. Boerckel [a,b], Nick J. Willett [a,b], Mon-Tzu A. Li [a,b], Nathaniel Huebsch [c,d], Robert E. Guldberg [a,b,*]

[a] Parker H. Petit Institute for Bioengineering & Bioscience, Georgia Institute of Technology, 315 Ferst Drive NW, Atlanta, GA 30332, USA
[b] George W. Woodruff School of Mechanical Engineering, Georgia Institute of Technology, 801 Ferst Drive NW, Atlanta, GA 303320, USA
[c] School of Engineering and Applied Sciences, Harvard University, 29 Oxford Street, Cambridge, MA 02138, USA
[d] Wyss Institute of Biologically Inspired Engineering, Harvard University, 60 Oxford Street, Cambridge, MA 02138, USA

ARTICLE INFO

*Article history:*
Received 6 March 2013
Revised 27 April 2013
Accepted 29 April 2013
Available online 7 May 2013

Edited by: Thomas Einhorn

*Keywords:*
Composite injury model
Bone defect
Ischemia
Bone regeneration
Vascularization
Bone morphogenetic protein

ABSTRACT

Although severe extremity trauma is often inclusive of skeletal and vascular damage in combination, segmental bone defect repair with concomitant vascular injury has yet to be experimentally investigated. To this end, we developed a novel rat composite limb injury model by combining a critically-sized segmental bone defect with surgically-induced hind limb ischemia (HLI). Unilateral 8 mm femoral defects were created alone (BD) or in combination with HLI (BD + HLI), and all defects were treated with rhBMP-2 via a hybrid biomaterial delivery system. Based on reported clinical and experimental observations on the importance of vascular networks in bone repair, we hypothesized that HLI would impair bone regeneration. Interestingly, the BD + HLI group displayed improved radiographic bridging, and quantitative micro-CT analysis revealed enhanced bone regeneration as early as week 4 ($p < 0.01$) that was sustained through week 12 ($p < 0.001$) and confirmed histologically. This effect was observed in two independent studies and at two different doses of rhBMP-2. Micro-CT angiography was used to quantitatively evaluate vascular networks at week 12 in both the thigh and the regenerated bone defect. No differences were found between groups in total blood vessel volume in the thigh, but clear differences in morphology were present as the BD + HLI group possessed a more interconnected network of smaller diameter vessels ($p < 0.001$). Accordingly, while the overall thigh vessel volume was comparable between groups, the contributions to vessel volume based on vessel diameter differed significantly. Despite this evidence of a robust neovascular response in the thigh of the BD + HLI group, differences were not observed between groups for bone defect blood vessel volume or morphology. In total, our results demonstrate that a transient ischemic insult and the subsequent recovery response to HLI significantly enhanced BMP-2-mediated segmental bone defect repair, providing additional complexity to the relationship between vascular tissue networks and bone healing. Ultimately, a better understanding of the coupling mechanisms may reveal important new strategies for promoting bone healing in challenging clinical scenarios.



## Introduction

Vascular tissues play an intricate role in many aspects of bone physiology, including bone repair. Blood vessel invasion is a critical step in developmental skeletogenesis as the cartilaginous intermediate is converted to bone [1,2]. Skeletal repair also recapitulates much of the developmental coupling of vascular and osseous growth [3]. A commendable amount of orthopaedic research has explored the role of angiogenesis in bone formation and repair, significantly advancing our understanding of angiogenic–osteogenic crosstalk. Angiogenesis is a necessary component in bone healing [4,5], and inhibition has experimentally been shown to disrupt both endochondral and intramembranous pathways of bone repair [6]. Beyond experimental results, clinical observations reinforce the importance of vasculature in bone healing. Diminished blood supply and concomitant vascular injury are clinical risk factors for delayed or nonunion fracture healing [7–9], while lower limb fractures with vascular injuries experience higher rates of amputation [10].

The deleterious effects of impaired vascular supply or concomitant vascular insult on clinical bone repair are certainly not surprising. Beyond the obvious physiological role of oxygen and nutrient transport, vascular networks likely also function as conduits for migrating inflammatory and progenitor cells as well as soluble factors essential for modulating the molecular signaling cascades of repair. Despite such a well-established understanding of the importance of adequate

* Corresponding author at: Georgia Institute of Technology, Parker H. Petit Institute for Bioengineering and Bioscience, 315 Ferst Drive NW, Atlanta, GA 30332, USA. Fax: +1 404 894 2291.
*E-mail address:* robert.guldberg@me.gatech.edu (R.E. Guldberg).

8756-3282/$ – see front matter © 2013 Elsevier Inc. All rights reserved.
http://dx.doi.org/10.1016/j.bone.2013.04.027

vascular networks for successful bone healing, only a few studies have investigated experimental bone repair with concomitant vascular injury [11,12], and none have involved bone defect repair. The lack of such research models is noteworthy, as extremity trauma with substantial skeletal damage is often accompanied by insults to the surrounding vasculature, and these injuries present unique and significant complications for clinicians [13]. Additionally, insufficient vascularization is an acknowledged shortcoming of status quo bone tissue engineering strategies [14,15], further complicating clinical treatment strategies. Continuing to unravel the complex interactions between vascular networks and bone regeneration will help to advance the design of therapeutic interventions for skeletal repair, and ultimately improve orthopaedic trauma patient treatment outcomes.

Accordingly, our aim here was to develop a rat model of composite lower limb bone and vascular trauma. To do so, we incorporated surgically-induced hind limb ischemia (HLI) with a well-established segmental bone defect model to evaluate the effects on bone repair. Such a model could provide new insights on interactions between bone healing and vascular tissues, as well as serve as a test bed for evaluating technologies to improve bone regeneration. Bone defects were treated using a previously reported recombinant human bone morphogenetic protein-2 (rhBMP-2) hybrid biomaterial delivery system [16–18]. This system has demonstrated efficacious bone regeneration, producing bone defect bridging with functional restoration. Based on reported clinical observations and experimental results, we hypothesized that HLI would impair bone regeneration in this model.

## Materials and methods

### *Experimental design*

The work described here consists of two independent experiments with pooled results. Thirteen-week-old female SASCO Sprague-Dawley rats (Charles River Laboratories) were designated for one of two injury model groups: 8 mm mid-femoral bone defects alone (BD) or in combination with hind limb ischemia (BD + HLI). The initial experiment consisted of $n = 10$ per group with each bone defect receiving a 2 μg rhBMP-2 treatment dose. This dose was chosen as it was previously shown to produce consistent bridging of defects in this model [17], but would not be so high as to overwhelm potential effects of HLI. A second experiment was performed to validate the findings of the first study at 2 μg rhBMP-2 ($n = 4$–5 per group) as well as evaluate a lower 0.5 μg treatment dose of rhBMP-2 previously shown to be inadequate for bone bridging ($n = 5$ per group) [17]. Within groups, no differences were found between experiments for the 2 μg dose, thus, results have been pooled for that dose level. All procedures were reviewed and approved by the Georgia Institute of Technology Institutional Animal Care and Use Committee and the United States Army Medical Research and Materiel Command Animal Care and Use Review Office.

### *Surgical procedure*

Animals were anesthetized via isoflurane inhalation and received unilateral surgeries to the left hind limb. The bone defect surgery and fixation were performed as described previously [19]. Briefly, a critically-sized 8 mm bone defect was created in the mid-diaphysis of the femur and stabilized by custom-made modular internal fixation plates with the use of miniature screws. The hind limb ischemia technique was adapted from methods previously described for mouse models [20,21]. Through an anterior skin incision, the femoral artery and vein were dissected free from associated nerves and ligated with 6-0 silk suture proximally at the inguinal ligament, distally at the popliteal bifurcation, and at two major arterial branch points in between. The length of the vessels between the inguinal ligament and popliteal bifurcation was then excised. Each bone defect was treated with a hybrid nanofiber mesh and RGD-functionalized alginate hydrogel rhBMP-2 delivery system previously described [16]. Briefly, a perforated, tubular electrospun nanofiber mesh was placed into the defect region such that it enveloped the cut ends of the native bone. A 150 μL volume of rhBMP-2-containing functionalized alginate hydrogel was then injected into the defect space (lumen of the nanofiber mesh). The rhBMP-2 treatment dose was 2 μg per defect, except where a lower 0.5 μg dose is indicated. Subcutaneous injections of buprenorphine were given for post-op analgesia. Animals were allowed access to food and water ad libitum, housed in a temperature and humidity controlled environment, and maintained on a 12:12 hour light/dark cycle.

### *Radiography*

Digital 2-D radiographs (Faxitron MX-20 Digital, Faxitron X-ray Corp.) were used for qualitative in vivo assessment of bone regeneration. Radiograph acquisition settings were 15 s exposure time at 25 kV. Radiograph imaging was performed at 2, 4, 8, and 12 weeks post-surgery. Bony bridging was evaluated in radiographs by three blinded investigators.

### *Microcomputed tomography*

In vivo micro-CT scans (vivaCT 40, Scanco Medical) were performed at 4, 8, and 12 weeks post-surgery to quantitatively assess 3-D bone regeneration. Legs were oriented along the z-axis and scanned with an applied electric potential of 55 kVp, a current of 109 μA, and an isometric voxel size of 38 μm. The volume of interest (VOI) for analysis was the center 5 mm (132 slices) of each defect. New mineral was segmented through application of a global threshold corresponding to 50% of native cortical bone density. A Gaussian low-pass filter was applied for noise suppression ($\sigma = 1.2$ and support $= 1$).

### *Micro-CT angiography*

At the week 12 study end-point, contrast agent-enhanced micro-CT angiography was used to quantitatively evaluate hind limb vasculature. The technique has been previously described in detail elsewhere [21,22]. Briefly, the vasculature was cleared with physiological saline containing 0.4% papaverine hydrochloride (Sigma-Aldrich), perfusion fixed with 10% neutral buffered formalin, rinsed again with physiological saline, and finally injected with lead chromate-based radiopaque contrast agent (2 parts Microfil MV-122: 1 part diluent, Flow Tech). Samples were stored at 4 °C overnight to allow for polymerization of the contrast agent. Hind limbs were excised and decalcified (Cal-Ex II, Fisher Scientific) over a period of 2–3 weeks under gentle agitation with routine solution changes.

Samples were oriented with the femur along the z-axis for micro-CT scanning (vivaCT 40, Scanco Medical). Two sets of scans and VOIs were used in this analysis. Initial scans were performed on the upper leg with an applied electric potential of 55 kVp, a current of 109 μA, and an isometric voxel size of 38 μm. The VOI for the initial set of scans consisted of the entirety of the cross-section of the leg spanning between the metal fixation plate components (Thigh VOI, refer to Fig. 5A for illustration). A second set of higher resolution scans focused on the defect region was performed with an isometric voxel size of 21 μm. The VOI for the second set of scans consisted of a cylindrical volume 5 mm in diameter that spanned the center 7 mm of the bone defect (Defect VOI). A global threshold was applied for segmentation of vasculature and a Gaussian low-pass filter was used for noise suppression ($\sigma = 0.8$ and support $= 1$).

*Histology*

Samples designated for histology were fixed in 10% neutral buffered formalin for 48 h at 4 °C and then decalcified (Cal-Ex II, Fisher Scientific) over a period of 2 weeks under gentle agitation with routine solution changes. Decalcified samples were paraffin processed and embedded. Longitudinal, 5 μm-thick sections were obtained from the central region of the defect, slide mounted, and stained with hematoxylin & eosin (H&E) or Safranin-O & fast green (Saf-O).

*Mechanical testing*

Explanted femora were mechanically tested to failure in torsion as previously described [19]. Briefly, excess soft tissue was carefully dissected from each sample, fixation hardware was removed, and femur ends were potted in custom blocks with Wood's metal (Alfa Aesar). Potted samples were mounted in torsion fixtures and rotated through failure at a ramp rate of 3°/s (Bose ELF 3200, Bose EnduraTEC). Rotation and torque data were recorded for each sample, from which maximum torque and torsional stiffness were determined.

*Data analysis*

All data are presented as mean ± standard error of the mean (SEM). Data were analyzed using analysis of variance (ANOVA) with Tukey's post-hoc test for pairwise comparisons or unpaired t-tests, as appropriate. The significance level was a $p$-value < 0.05. All data analysis was performed in Minitab 15 (Minitab, Inc.) or GraphPad Prism 5 (GraphPad Software, Inc.).

## Results

All operated animals tolerated the initial surgical procedure well and returned to normal activity. A small number of samples were excluded from the study due to abscess formation at the defect, unstable fixation, or additional bone fracture (3 animals in total). Successful induction of ischemia was demonstrated in a separate experiment (Supplementary material, Fig. S1).

*Higher rhBMP-2 dose bone regeneration*

At the 2 μg rhBMP-2 dose, digital 2-D radiographs displayed qualitatively similar bone regeneration between groups across the 2, 4, 8, and 12 week time points examined (Fig. 1A). Overall, 11 of 13 defects in the BD group went on to bony bridging. In the BD + HLI group, all 15 defects achieved bridging.

Interestingly, micro-CT analysis quantitatively demonstrated a significant increase in the amount of regenerated bone for the BD + HLI group compared to BD alone (Figs. 1B & C). The increase was evident as early as week 4 ($p < 0.01$, 53% increase), and was sustained through week 12 ($p < 0.001$, 44% increase).

Micro-CT results were further corroborated with histological analysis performed at week 12. H&E stained tissue sections displayed qualitatively more robust bone formation in the defects of the BD + HLI group compared to BD alone (Figs. 2A & B). Bone formation at the periphery of the defect (along the nanofiber mesh) was similarly robust in both groups (Figs. 2C & F). Differences were apparent in the central region of defects, however, with the BD + HLI group possessing qualitatively more bone tissue and less fibrous tissue (Figs. 2D, E, G & H). In both groups, small pockets of alginate persisted at week 12. Safranin-O staining was used to assess cartilage composition in repaired defects. Small pockets of cartilage persisted in each group, but no notable differences between groups were observed (Fig. S2).

Torsional testing to failure was used to assess functional restoration of the regenerated bone at week 12. The BD + HLI group exhibited greater maximum torque (77% increase) and torsional stiffness (59% increase) compared to the BD group (Fig. 3), but differences were not

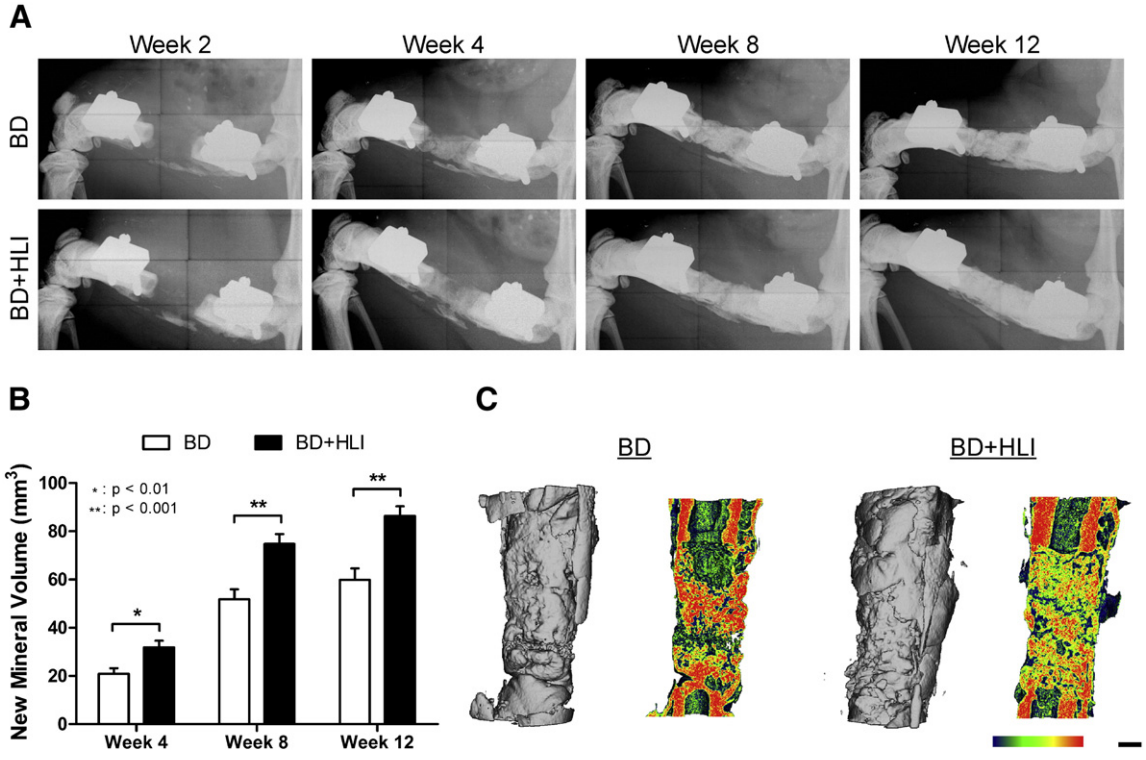


**Fig. 1.** Longitudinal analysis of bone regeneration. (A) Representative digital radiographs acquired at post-surgery weeks 2, 4, 8, and 12. (B) Quantification of new mineral volume in the defect obtained from longitudinal in vivo micro-CT scans. (C) Representative 3D reconstructions of ex vivo micro-CT scans with cross-sectional mineral density maps. Native cortical bone ends have been included for reference. Scale bars: density = 2.5–5 1/cm, length = 1 mm. *: $p < 0.01$, **: $p < 0.001$. n = 13–15 per group.

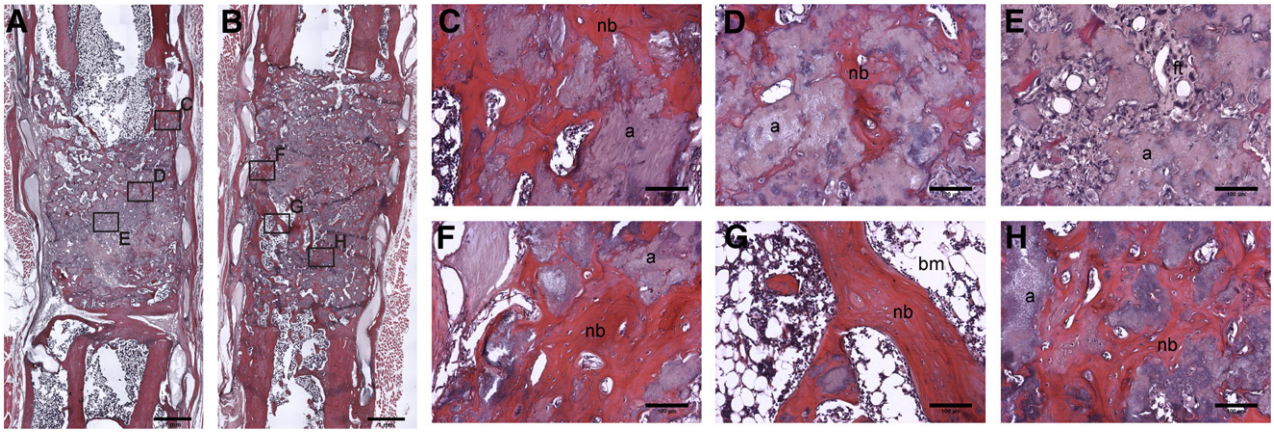


**Fig. 2.** H&E histology of bone healing at 12 weeks. (A, B) Mosaic images of H&E stained mid-defect sagittal sections from the BD (A) and BD + HLI (B) groups confirmed increased bone regeneration in BD + HLI group. (C–H) Higher magnification fields from mosaic images demonstrating more robust bone formation in BD + HLI group. Magnification = 4× (A, B) and 10× (C–H). Scale bars = 1 mm (A, B) and 100 μm (C–H). Annotations: a = alginate, bm = bone marrow, ft = fibrous tissue, nb = new bone.

statistically significant ($p = 0.214$ and $p = 0.434$, respectively). Compared to historical data of age-matched, naïve intact femur controls (maximum torque = 0.31 ± 0.04 N∗m, torsional stiffness = 0.030 ± 0.003 N∗m/deg, n = 6 [16]), the BD group achieved only 42% of maximum torque and 77% of torsional stiffness, whereas the BD + HLI group achieved 74% of maximum torque and 123% of torsional stiffness.

*Lower rhBMP-2 dose bone regeneration*

To further investigate these findings, an experiment was conducted using a lower 0.5 μg treatment dose of BMP-2, a dose previously demonstrated to be insufficient for consistent bridging [17]. In agreement with the findings at 2 μg dose, improved bone healing was observed in the BD + HLI group. Radiograph evaluation determined only 2 of 4 defects in the BD group achieved bony bridging; in contrast bridging was achieved in 4 of 4 BD + HLI samples (Fig. 4A). Micro-CT results also showed an increase in regenerated bone volume in the BD + HLI group compared to BD alone, but did not reach statistical significance ($p = 0.069$ and 67% increase at week 12, Figs. 4A & B). Torsional testing revealed additional differences between groups (Fig. 4C), as the BD + HLI group displayed significantly increased maximum torque ($p < 0.05$, 118% increase) and a nearly 14-fold increase in torsional stiffness ($p = 0.1146$, 1382% increase). Compared to historical data of age-matched, naïve intact femur controls (maximum torque = 0.31 ± 0.04 N∗m, torsional stiffness = 0.030 ± 0.003 N∗m/deg, n = 6 [16]), the BD group achieved only 19% of maximum torque and 7% of torsional stiffness, whereas the BD + HLI group achieved 42% of maximum torque and 83% of torsional stiffness.

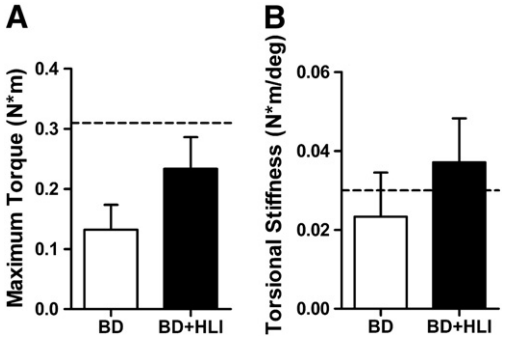


**Fig. 3.** Torsional testing mechanical properties of regenerated bone at 12 weeks. (A) Maximum torque to failure and (B) torsional stiffness. Dashed lines indicate mean values for historical naïve intact controls [16]. n = 3–4 per group.

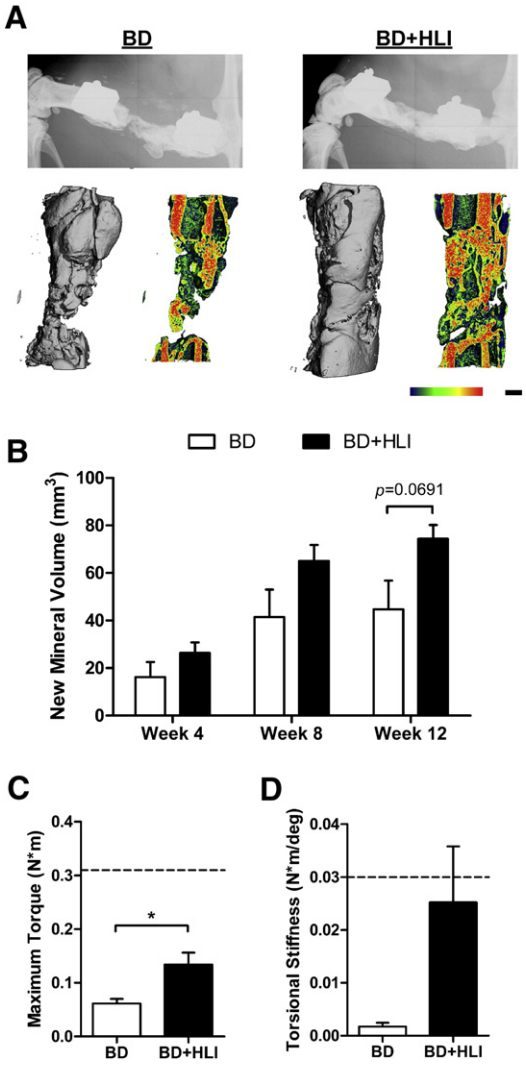


**Fig. 4.** Bone repair at lower 0.5 μg rhBMP-2 dose. (A) Representative digital radiographs from week 12 and 3D micro-CT reconstructions with mineral density mapping. (B) Quantification of new mineral volume in the defect obtained from longitudinal in vivo micro-CT scans. (C) Maximum torque to failure and (D) torsional stiffness. Dashed lines indicate mean values for historical naïve intact controls [16]. Scale bars: density = 2.5–5 1/cm, length = 1 mm. *: $p < 0.05$. n = 3–4 per group.

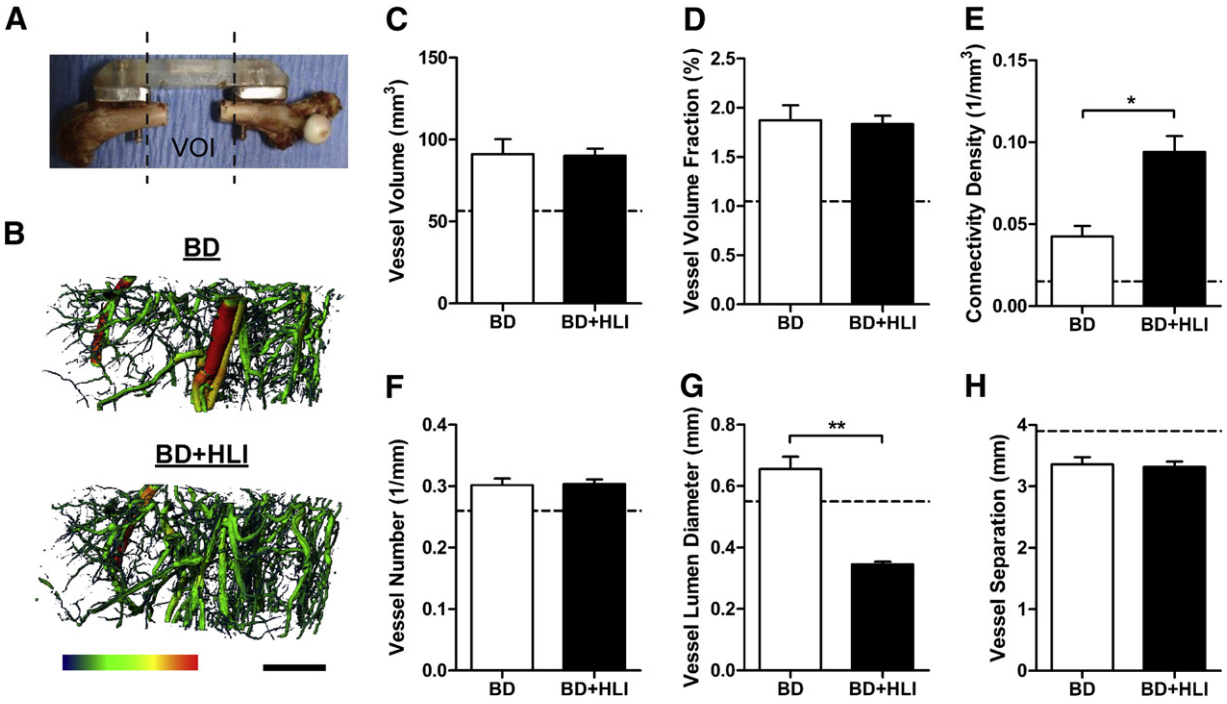


**Fig. 5.** Thigh blood vessel volume and morphology at week 12. (A) Illustration of thigh VOI. (B) Representative 3D micro-CT reconstructions with vessel diameter mapping. (C–H) Angiography parameters in the thigh VOI: blood vessel volume (C), tissue vessel volume fraction (D), connectivity density (E), mean vessel number (F), mean vessel lumen diameter (G), and mean vessel separation (H). Dashed lines indicate mean values for contralateral controls. Scale bars: diameter 0–1 mm, length = 5 mm. *: $p < 0.001$, **: $p < 0.0001$. n = 8 per group.

*Vascular networks*

A micro-CT angiography technique was used at week 12 to quantitatively evaluate vascular volume and morphology. In the Thigh VOI (Figs. 5A & B), no differences in vessel volume or vessel volume fraction were evident between groups (Figs. 5C & D), suggesting a robust neovascular recovery response and only transient ischemia. Morphological differences were observed, however, with a more interconnected ($p < 0.001$) network of smaller diameter ($p < 0.0001$) vessels apparent in the BD + HLI group compared to BD alone (Figs. 5E–H). Compared to contralateral controls, both groups exhibited an approximately 60% increase in vessel volume. Both groups also showed increased vessel connectivity and number of vessels, with a decrease in vessel separation. The BD group exhibited an increase in mean vessel diameter compared to contralateral controls, while the BD + HLI group was decreased.

Voxel count histograms provided an indication of vessel size frequency distribution. The BD + HLI group displayed a distribution skewed toward smaller diameter vessels, with an increase in vessels of luminal diameter less than ~500 μm and a lack of vessels with luminal diameter greater than ~1 mm (Fig. 6A). Furthermore, while the overall vessel volume was comparable between groups, the contributions to vessel volume based on vessel diameter were significantly different between groups (Fig. 6B). Specifically, the BD + HLI group had a significantly greater contribution from vessels with diameters of ~200–500 μm compared to BD alone ($p < 0.005$) and significantly less contribution from vessels with diameter larger than ~1 mm ($p < 0.0001$). While contributions to vessel volume were rather uniform in the BD group (22%–28% across the 4 bins of analysis), 75% of vessel volume in the BD + HLI group came from vessels with diameter less than ~500 μm (Fig. 6C).

Analysis of the defect VOI revealed no differences between groups in terms of blood vessel volume or morphology (Fig. 7).

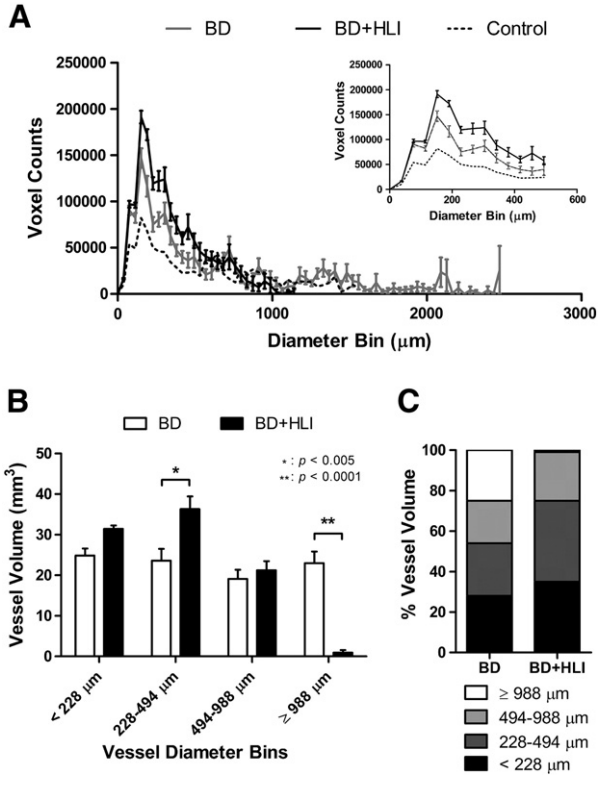


**Fig. 6.** Thigh blood vessel diameter frequency distributions and contributions to vessel volume at week 12. (A) Frequency distribution of blood vessel voxel sizes from the thigh VOI that give a representative distribution of blood vessel diameter. (Inset) Magnification of the 0–494 μm bins. (B) Contributions to blood vessel volume from different vessel diameter ranges. (C) Contributions to vessel volume expressed as a percent of total vessel volume. *: $p < 0.005$, **: $p < 0.0001$. n = 8 per group.

## Discussion

The established relationships between vascular tissues and bone repair provide compelling motivation for new research models to

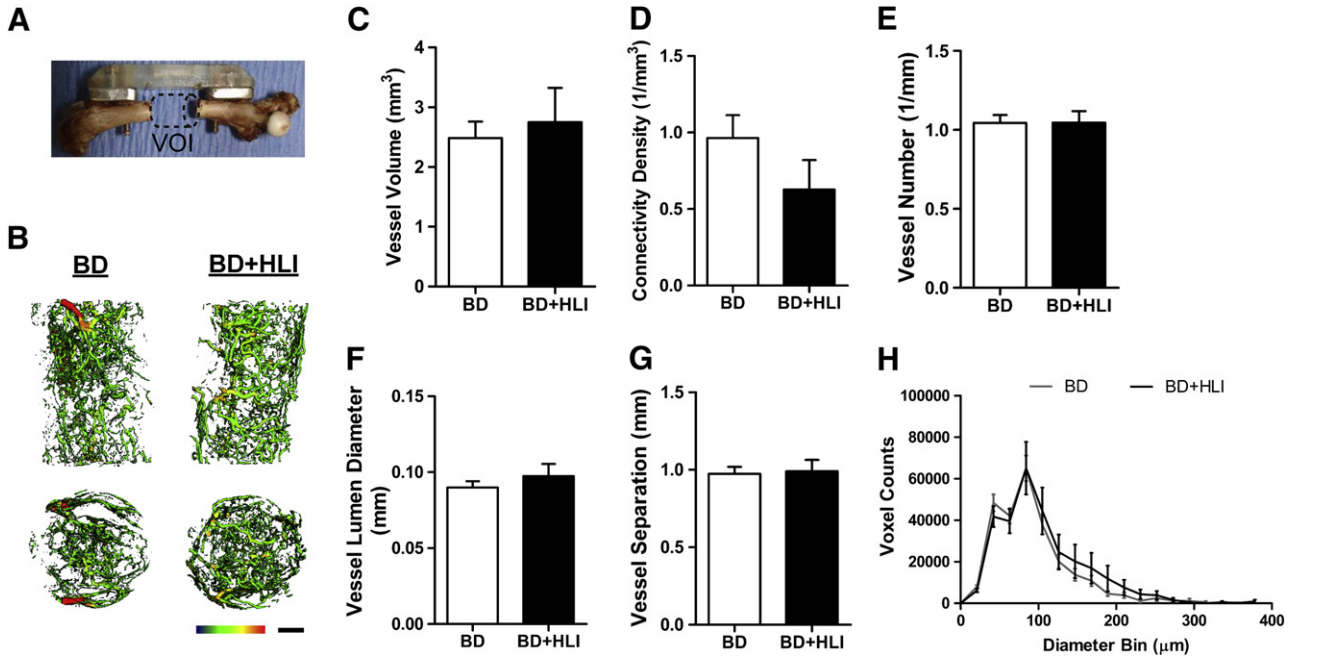


**Fig. 7.** Bone defect blood vessel volume and morphology at week 12. (A) Illustration of defect VOI. (B) Representative 3D micro-CT reconstructions with vessel diameter mapping. Side views (upper) and proximal top down views (lower) of the cylindrical volume are shown. (C–H) Angiography parameters in the Defect VOI: blood vessel volume (C), connectivity density (D), mean vessel number (E), mean vessel lumen diameter (F), mean vessel separation (G), and vessel diameter frequency distribution (H). Scale bars: diameter 0–200 μm, length = 1 mm. n = 8 per group.

advance our understanding of the coupling mechanisms, as well as methods to improve treatment for orthopaedic trauma patients with concomitant vascular insults. Here we sought to address the specific lack of a small animal model of severe composite bone and vascular trauma by pairing a critically-sized mid-femoral defect with surgically-induced hind limb ischemia in the rat. Interestingly, our data did not support our original hypothesis, as recovery from transient HLI enhanced bone regeneration compared to bone defects without concomitant vascular injury. These observations were both repeatable and robust across varying levels of rhBMP-2 stimulation. Although initially unexpected, these findings are notable, and understanding the underlying mechanisms may have important implications for clinical therapeutics.

Bone regeneration and mechanical properties for the BD group here were consistent with previously published data for both the 2 μg and 0.5 μg rhBMP-2 doses [16,17]. Importantly, with no treatment, or vehicle alone, these defects will not heal and reliably progress to non-union [16,19]. One of the most interesting observations here was the transformation of the non-healing 0.5 μg rhBMP-2 dose to a healing one with concomitant HLI. In general, bone healing in the BD + HLI group was comparable with results historically observed in bone defects treated with higher rhBMP-2 doses (e.g., 2 μg similar to 5 μg; 0.5 μg similar to 1–2.5 μg) [16,17]. These historical comparisons were consistent with the results here, as both bone regeneration and mechanical properties for the 0.5 μg BD + HLI group were comparable to those of the 2 μg BD group. This is an interesting point for future consideration given the high costs and incompletely understood (and at times negative) effects associated with current supraphysiologic doses of BMPs administered to human patients [23–26]. Furthermore, the delivery hydrogel used here provides more prolonged growth factor release kinetics than the clinical gold standard for rhBMP-2 delivery (absorbable collagen sponge) [16,17], which may be important in allowing for crosstalk between vascular growth processes and bone repair. In addition, given the wide variety of physiological processes that BMP-2 has been implicated in, including blood vessel growth and remodeling [27,28], it is conceivable that in this specific model the rhBMP-2 provided an additional indirect bone healing stimulus by augmenting the vascular tissue response to ischemia. A better understanding of the coupling mechanisms involved in the model presented here may produce new therapeutic strategies that would allow for lower doses of rhBMP-2 to be used in humans without sacrificing efficacy.

One potential explanation for the enhanced bone regeneration in the BD + HLI group is a robust endogenous vascular response to ischemia. While the HLI surgical procedure was demonstrated to effectively create an initial substantial reduction in perfusion of the leg, it is understood from other work that this is a transient effect due primarily to arteriogenic growth of collateral vessels in the limb [20,21]. Murine models of HLI are widely used in the field of vascular biology and recovery from HLI induced by femoral artery ligation has been shown to be background strain dependent in mice, ranging from necrosis of the limb to restoration of perfusion within a few days [29]. In rat models of femoral artery ligation, restoration of resting perfusion appears to possess an intermediate recovery length, having been reported at 5–7 days [30,31]. Deficits in reserve blood flow have longer duration, extending beyond 14 days [31], and it is unknown what influence a concomitant orthopaedic injury may have on the recovery time. As evidenced by the micro-CT angiography results, blood vessel volume was not different between groups at week 12. One limitation of the micro-CT angiography technique (as with other angiography techniques), however, is an inability to distinguish between arterial and venous supply, perhaps obscuring important insights regarding vascular networks. Vessels with luminal diameters larger than 1 mm are almost exclusively the femoral artery and vein (especially the latter). This vessel size range exhibited significantly different contributions to vessel volume between groups (25% for BD, 1% for BD + HLI). The fact that the femoral vessels were excised in the BD + HLI group, yet no differences in total blood vessel volume were observed, may suggest increased arterial blood supply to the thigh in this group. The increases in vessel volume, connectivity, number of vessels, and decrease in vessel separation in each group compared to contralateral controls is an expected wound healing response. Whereas the BD + HLI group

exhibited a decrease in mean vessel lumen diameter compared to contralateral controls, the BD group actually exhibited an increase. This may be indicative of vasodilation of vessels in this group or some degree of arteriogenesis. Importantly, the results presented here provide only a single snapshot of post-injury blood vessel growth and remodeling at the week 12 end point, and do not preclude additional differences at earlier time points. Ongoing experiments are studying vessel networks early in the healing process in order to provide additional insight into the transient response characteristics and to better interpret these results.

Post-injury vascular growth in this model likely occurs through a combination of angiogenesis and arteriogenesis. Angiogenesis is understood to be an essential component to the bone healing processes [4,5]. Previous work has demonstrated the role of hypoxia inducible transcription factor-1α (HIF-1α), an angiogenic transcription factor under inhibitory control in normoxic conditions, in coupling angiogenesis and osteogenesis during bone repair primarily through a VEGF-mediated mode of action [32,33]. The HLI surgery may affect tissue oxygen tension which would implicate a role for HIF-1α and VEGF in the results observed here. Endogenous VEGF is known to be essential in both intramembranous and endochondral bone healing processes, and delivery of exogenous VEGF has been shown to improve fracture and bone defect repair [6]. VEGF may also up-regulate BMP-2 expression in vascular tissues via paracrine signaling [34,35] or act through direct binding with osteoblast VEGF receptors [36,37].

Arteriogenesis offers a viable additional, if not alternative, method of augmented post-injury vascular growth. In small animal models of HLI, the upper leg is thought to primarily undergo arteriogenic growth of collateral arteries due to increased shear stress experienced by arterioles as they attempt to compensate for greater blood flow demands, whereas the lower leg primarily experiences angiogenesis in response to hypoxia [38]. This would seem to imply that although new vessel formation in the bone defect may be due to angiogenesis, arteriogenesis may be the predominant vascular tissue growth process in our model; however, a direct role for arteriogenesis in bone repair is not yet well-defined. In agreement with this hypothesis, recent work from Morgan et al. demonstrated that the vascular growth associated with distraction osteogenesis is characterized by initial arteriogenic remodeling of vessels in the surrounding skeletal muscle compartment with subsequent vessel ingrowth to the regenerating distraction space [39].

It is also possible that HLI augments the gene expression, soluble factor bioavailability, cellular populations mobilized to the injury site and surrounding areas, or some combination thereof. In this way, the endogenous vascular response to HLI may play more of an indirect role in enhancing the bone repair process in the BD + HLI group as opposed to exerting a direct influence. The extracellular matrix protein osteopontin is significantly up-regulated in response to HLI [40], plays a definitive role in collateral vessel development and recovery from ischemia [41], and is involved in regulating several aspects of fracture healing [42]. Other growth factors associated with arteriogenesis such as platelet derived growth factor, transforming growth factor-β, and fibroblast growth factor-2 [43], have also been implicated in bone regeneration [44], and provide additional means of molecular cross-talk in these processes. At a cellular level, monocyte/macrophage invasion plays a significant role in collateral vessel growth following arterial occlusion [45]. Arteriogenic macrophages have been reported to be of an M2/wound-healing phenotype [46], and macrophages may possess a capacity for osteoinductive signaling through BMP-2 secretion [47]. Through such mechanisms, activation or mobilization of an augmented macrophage population due to concomitant HLI may have had downstream effects on bone repair in our model. Vascular smooth muscle cells (SMC) also play a critical cellular role in arteriogenic vessel remodeling, with phenotypic changes and proliferation initiating early in the process [38]. Additionally, SMCs are considered at least partially responsible for vascular tissue calcification [48], potentially in a process also involving macrophages [48,49]. Pericytes, which are more commonly associated with the microvessels, may also play some role in the bone regeneration results observed here as a perivascular source of osteoprogenitor cells [50–52].

Consideration should also be given to the role that the surrounding skeletal muscle envelope plays in this model, given that at the very least it is the site of extensive vascular growth and remodeling. In related work, our group recently demonstrated that volumetric muscle loss attenuated rhBMP-2-mediated segmental bone defect repair in a rat model of composite bone and skeletal muscle injury [53]. This effect is thought to be at least partially attributable to diminished vascular growth, but may also involve reduced availability of skeletal muscle resident osteoprogenitor cells and cytokines/growth factors involved in transmitting the necessary signaling cascades—factors that could also be affected by HLI.

To our knowledge, the work here is the first to combine segmental bone defect repair with concomitant vascular injury. Two previously published models have investigated fracture healing in combination with an ischemic injury. Lu et al. found that ischemia induced by femoral artery resection impaired healing of murine tibial fractures, with reduced blood vessels in and around ischemic leg fractures [12]. Kase et al. reported no differences in rat tibial fracture healing when acute ischemia/reperfusion was incorporated via tourniquet and microvascular clip application/removal [11]. The disparity in results from those two studies is most likely attributable to the varying degrees of ischemia induced. The model of Lu et al. is most similar to our own, with the inverse bone repair findings perhaps resulting from the location of orthopaedic injury, and the implications this would have on the relevant vascular growth processes. In our model, the bone defect is adjacent to the vascular injury by design in order to mimic a localized injury, whereas in the model of Lu et al., the fracture is further downstream of the vascular injury, perhaps producing a more hypoxic environment. The other confounding factor between the models is the rhBMP-2 delivery included here. Interestingly, in a follow-up study, Lu et al. found that delivery of rhBMP-7 improved ischemic fracture healing and was associated with increased tissue vascularity [54].

Overall, our results did not validate our original hypothesis and suggest that this model does not recapitulate complications associated with vascular compromised clinical bone healing. This is most likely due to differences in scale of human patients versus small animal models, and the observation that the rat HLI injury induced a robust vascular response and only transient limb ischemia. However, the unexpected results of this study are important as they shed further light on the complex interactions between bone healing and vascular tissue growth. Future work to improve understanding of the underlying mechanisms could provide useful insight to exploit this interaction and guide development of novel therapeutic strategies for challenging clinical bone healing scenarios.

## Conclusions

Bone repair is intimately linked to vascular growth and remodeling processes. Here we describe a novel model of composite tissue trauma combining a segmental bone defect with concomitant vascular injury. Contrary to our original hypothesis, our results demonstrated that the recovery response to HLI significantly enhanced BMP-2-mediated segmental bone defect repair in this model. Despite a robust neovascular response in the thigh of the group with HLI, differences were not observed between groups for bone defect blood vessel volume and morphology. These results suggest additional mechanisms of interaction beyond the direct vascular response, perhaps inclusive of augmented cellular exchange, gene expression, soluble factor availability, or some combination thereof. In sum, the work presented here provides additional complexity to the relationship between vascular tissues and bone healing, and a better understanding of the associated coupling mechanisms may reveal important new strategies for promoting bone healing.

## Acknowledgements

This work was supported by the Armed Forces Institute of Regenerative Medicine (AFIRM). The authors would like to thank Dr. David Mooney for useful discussions regarding preparation of the RGD-modified alginate, Dr. Natalia Landázuri for assistance with adapting the hind limb ischemia surgery technique, and Dr. Laura O'Farrell for veterinary assistance. Additional thanks to Hazel Stevens, Angela Lin, Ashley Allen, Dr. Tamim Diab, Christopher Dosier, Taran Lundgren, Lauren Priddy, and Tanushree Thote for their assistance during surgeries.

## Appendix A. Supplementary data

Supplementary data to this article can be found online at http://dx.doi.org/10.1016/j.bone.2013.04.027.

## References

[1] Gerber HP, Vu TH, Ryan AM, Kowalski J, Werb Z, Ferrara N. VEGF couples hypertrophic cartilage remodeling, ossification and angiogenesis during endochondral bone formation. Nat Med 1999;5:623–8.
[2] Kronenberg HM. Developmental regulation of the growth plate. Nature 2003;423:332–6.
[3] Ferguson C, Alpern E, Miclau T, Helms JA. Does adult fracture repair recapitulate embryonic skeletal formation? Mech Dev 1999;87:57–66.
[4] Glowacki J. Angiogenesis in fracture repair. Clin Orthop Relat Res 1998:S82–9.
[5] Carano RA, Filvaroff EH. Angiogenesis and bone repair. Drug Discov Today 2003;8:980–9.
[6] Street J, Bao M, deGuzman L, Bunting S, Peale Jr FV, Ferrara N, et al. Vascular endothelial growth factor stimulates bone repair by promoting angiogenesis and bone turnover. Proc Natl Acad Sci U S A 2002;99:9656–61.
[7] Einhorn TA. Enhancement of fracture-healing. J Bone Joint Surg Am 1995;77:940–56.
[8] Brinker MR, Bailey Jr DE. Fracture healing in tibia fractures with an associated vascular injury. J Trauma 1997;42:11–9.
[9] Dickson K, Katzman S, Delgado E, Contreras D. Delayed unions and nonunions of open tibial fractures. Correlation with arteriography results. Clin Orthop Relat Res 1994:189–93.
[10] Glass GE, Pearse MF, Nanchahal J. Improving lower limb salvage following fractures with vascular injury: a systematic review and new management algorithm. J Plast Reconstr Aesthet Surg 2009;62:571–9.
[11] Kase T, Skjeldal S, Nordsletten L, Reikeras O. Healing of tibial fractures is not impaired after acute hindlimb ischemia in rats. Arch Orthop Trauma Surg 1998;117:273–6.
[12] Lu C, Miclau T, Hu D, Marcucio RS. Ischemia leads to delayed union during fracture healing: a mouse model. J Orthop Res 2007;25:51–61.
[13] Nauth A, McKee MD, Einhorn TA, Watson JT, Li R, Schemitsch EH. Managing bone defects. J Orthop Trauma 2011;25:462–6.
[14] Muschler GF, Nakamoto C, Griffith LG. Engineering principles of clinical cell-based tissue engineering. J Bone Joint Surg Am 2004;86-A:1541–58.
[15] Kanczler JM, Oreffo RO. Osteogenesis and angiogenesis: the potential for engineering bone. Eur Cell Mater 2008;15:100–14.
[16] Kolambkar YM, Dupont KM, Boerckel JD, Huebsch N, Mooney DJ, Hutmacher DW, et al. An alginate-based hybrid system for growth factor delivery in the functional repair of large bone defects. Biomaterials 2011;32:65–74.
[17] Boerckel JD, Kolambkar YM, Dupont KM, Uhrig BA, Phelps EA, Stevens HY, et al. Effects of protein dose and delivery system on BMP-mediated bone regeneration. Biomaterials 2011;32:5241–51.
[18] Kolambkar YM, Boerckel JD, Dupont KM, Bajin M, Huebsch N, Mooney DJ, et al. Spatiotemporal delivery of bone morphogenetic protein enhances functional repair of segmental bone defects. Bone 2011;49:485–92.
[19] Oest ME, Dupont KM, Kong HJ, Mooney DJ, Guldberg RE. Quantitative assessment of scaffold and growth factor-mediated repair of critically sized bone defects. J Orthop Res 2007;25:941–50.
[20] Couffinhal T, Silver M, Zheng LP, Kearney M, Witzenbichler B, Isner JM. Mouse model of angiogenesis. Am J Pathol 1998;152:1667–79.
[21] Duvall CL, Taylor WR, Weiss D, Guldberg RE. Quantitative microcomputed tomography analysis of collateral vessel development after ischemic injury. Am J Physiol Heart Circ Physiol 2004;287:H302–10.
[22] Boerckel JD, Uhrig BA, Willett NJ, Huebsch N, Guldberg RE. Mechanical regulation of vascular growth and tissue regeneration in vivo. Proc Natl Acad Sci U S A 2011;108:E674–80.
[23] Garrison KR, Donell S, Ryder J, Shemilt I, Mugford M, Harvey I, et al. Clinical effectiveness and cost-effectiveness of bone morphogenetic proteins in the non-healing of fractures and spinal fusion: a systematic review.Health Technol Assess 2007;11:1–150 iii–iv.
[24] Cahill KS, Chi JH, Day A, Claus EB. Prevalence, complications, and hospital charges associated with use of bone-morphogenetic proteins in spinal fusion procedures. JAMA 2009;302:58–66.
[25] Devine JG, Dettori JR, France JC, Brodt E, McGuire RA. The use of rhBMP in spine surgery: is there a cancer risk? Evid Based Spine Care J 2012;3:35–41.
[26] Even J, Eskander M, Kang J. Bone morphogenetic protein in spine surgery: current and future uses. J Am Acad Orthop Surg 2012;20:547–52.
[27] Deckers MM, van Bezooijen RL, van der Horst G, Hoogendam J, van Der Bent C, Papapoulos SE, et al. Bone morphogenetic proteins stimulate angiogenesis through osteoblast-derived vascular endothelial growth factor A. Endocrinology 2002;143:1545–53.
[28] Langenfeld EM, Langenfeld J. Bone morphogenetic protein-2 stimulates angiogenesis in developing tumors. Mol Cancer Res 2004;2:141–9.
[29] Helisch A, Wagner S, Khan N, Drinane M, Wolfram S, Heil M, et al. Impact of mouse strain differences in innate hindlimb collateral vasculature. Arterioscler Thromb Vasc Biol 2006;26:520–6.
[30] Seifert FC, Banker M, Lane B, Bagge U, Anagnostopoulos CE. An evaluation of resting arterial ischemia models in the rat hind limb. J Cardiovasc Surg (Torino) 1985;26:502–8.
[31] Corcoran HA, Smith BE, Mathers P, Pisacreta D, Hershey JC. Laser Doppler imaging of reactive hyperemia exposes blood flow deficits in a rat model of experimental limb ischemia. J Cardiovasc Pharmacol 2009;53:446–51.
[32] Wan C, Gilbert SR, Wang Y, Cao X, Shen X, Ramaswamy G, et al. Activation of the hypoxia-inducible factor-1alpha pathway accelerates bone regeneration. Proc Natl Acad Sci U S A 2008;105:686–91.
[33] Schipani E, Maes C, Carmeliet G, Semenza GL. Regulation of osteogenesis–angiogenesis coupling by HIFs and VEGF. J Bone Miner Res 2009;24:1347–53.
[34] Bouletreau PJ, Warren SM, Spector JA, Peled ZM, Gerrets RP, Greenwald JA, et al. Hypoxia and VEGF up-regulate BMP-2 mRNA and protein expression in microvascular endothelial cells: implications for fracture healing. Plast Reconstr Surg 2002;109:2384–97.
[35] Matsubara H, Hogan DE, Morgan EF, Mortlock DP, Einhorn TA, Gerstenfeld LC. Vascular tissues are a primary source of BMP2 expression during bone formation induced by distraction osteogenesis. Bone 2012;51:168–80.
[36] Deckers MM, Karperien M, van der Bent C, Yamashita T, Papapoulos SE, Lowik CW. Expression of vascular endothelial growth factors and their receptors during osteoblast differentiation. Endocrinology 2000;141:1667–74.
[37] Clarkin CE, Gerstenfeld LC. VEGF and bone cell signalling: an essential vessel for communication? Cell Biochem Funct 2013;31:1–11.
[38] Schaper W, Scholz D. Factors regulating arteriogenesis. Arterioscler Thromb Vasc Biol 2003;23:1143–51.
[39] Morgan EF, Hussein AI, Al-Awadhi BA, Hogan DE, Matsubara H, Al-Alq Z, et al. Vascular development during distraction osteogenesis proceeds by sequential intramuscular arteriogenesis followed by intraosteal angiogenesis. Bone 2012;51:535–45.
[40] Lyle AN, Joseph G, Fan AE, Weiss D, Landazuri N, Taylor WR. Reactive oxygen species regulate osteopontin expression in a murine model of postischemic neovascularization. Arterioscler Thromb Vasc Biol 2012;32:1383–91.
[41] Duvall CL, Weiss D, Robinson ST, Alameddine FM, Guldberg RE, Taylor WR. The role of osteopontin in recovery from hind limb ischemia. Arterioscler Thromb Vasc Biol 2008;28:290–5.
[42] Duvall CL, Taylor WR, Weiss D, Wojtowicz AM, Guldberg RE. Impaired angiogenesis, early callus formation, and late stage remodeling in fracture healing of osteopontin-deficient mice. J Bone Miner Res 2007;22:286–97.
[43] Buschmann I, Heil M, Jost M, Schaper W. Influence of inflammatory cytokines on arteriogenesis. Microcirculation 2003;10:371–9.
[44] Kempen DH, Creemers LB, Alblas J, Lu L, Verbout AJ, Yaszemski MJ, et al. Growth factor interactions in bone regeneration. Tissue Eng Part B Rev 2010;16:551–66.
[45] Arras M, Ito WD, Scholz D, Winkler B, Schaper J, Schaper W. Monocyte activation in angiogenesis and collateral growth in the rabbit hindlimb. J Clin Invest 1998;101:40–50.
[46] Takeda Y, Costa S, Delamarre E, Roncal C, Leite de Oliveira R, Squadrito ML, Finisguerra V, Deschoemaeker S, Bruyere F, Wenes M, Hamm A, Serneels J, Magat J, Bhattacharyya T, Anisimov A, Jordan BF, Alitalo K, Maxwell P, Gallez B, Zhuang ZW, Saito Y, Simons M, De Palma M, Mazzone M. Macrophage skewing by Phd2 haplodeficiency prevents ischaemia by inducing arteriogenesis. Nature 2011;479:122–6.
[47] Champagne CM, Takebe J, Offenbacher S, Cooper LF. Macrophage cell lines produce osteoinductive signals that include bone morphogenetic protein-2. Bone 2002;30:26–31.
[48] Trion A, van der Laarse A. Vascular smooth muscle cells and calcification in atherosclerosis. Am Heart J 2004;147:808–14.
[49] Ikeda K, Souma Y, Akakabe Y, Kitamura Y, Matsuo K, Shimoda Y, et al. Macrophages play a unique role in the plaque calcification by enhancing the osteogenic signals exerted by vascular smooth muscle cells. Biochem Biophys Res Commun 2012;425:39–44.
[50] Towler DA. Vascular biology and bone formation: hints from HIF. J Clin Invest 2007;117:1477–80.
[51] Crisan M, Yap S, Casteilla L, Chen CW, Corselli M, Park TS, et al. A perivascular origin for mesenchymal stem cells in multiple human organs. Cell Stem Cell 2008;3:301–13.
[52] Caplan AI, Correa D. PDGF in bone formation and regeneration: new insights into a novel mechanism involving MSCs. J Orthop Res 2011;29:1795–803.
[53] Willett NJ, Li MT, Uhrig BA, Boerckel JD, Huebsch N, Lundgren TL, Warren GL, Guldberg RE. Attenuated human bone morphogenetic protein-2-mediated bone regeneration in a rat model of composite bone and muscle injury. Tissue Eng Part C Methods 2013;19(4):316–25.
[54] Lu C, Xing Z, Yu YY, Colnot C, Miclau T, Marcucio RS. Recombinant human bone morphogenetic protein-7 enhances fracture healing in an ischemic environment. J Orthop Res 2010;28:687–96.